Supporting information for

On the Absence of Triplet Exciton Loss Pathways in Non-Fullerene Acceptor based Organic Solar Cells

Maria S. Kotova[1], Giacomo Londi[2], Johannes Junker[1], Stefanie Dietz[1], Alberto Privitera[3], Kristofer Tvingstedt[1], David Beljonne[2], Andreas Sperlich[1*] and Vladimir Dyakonov[1]

[1]Experimental Physics 6, Julius Maximilian University of Würzburg, Am Hubland, 97074 Würzburg, Germany

[2] Laboratory for Chemistry of Novel Materials, University of Mons, B-7000 Mons, Belgium

[3] Clarendon Laboratory, Department of Physics, University of Oxford, Oxford OX1 3PU, England, UK

Device optimization

Optimization details and corresponding performance parameters of the PBDB-T:ITIC-based OSCs under AM 1.5G illumination (100 mW cm^{-2}). Solar cell preparation was tested with and without the additive di-iodooctane (DIO).

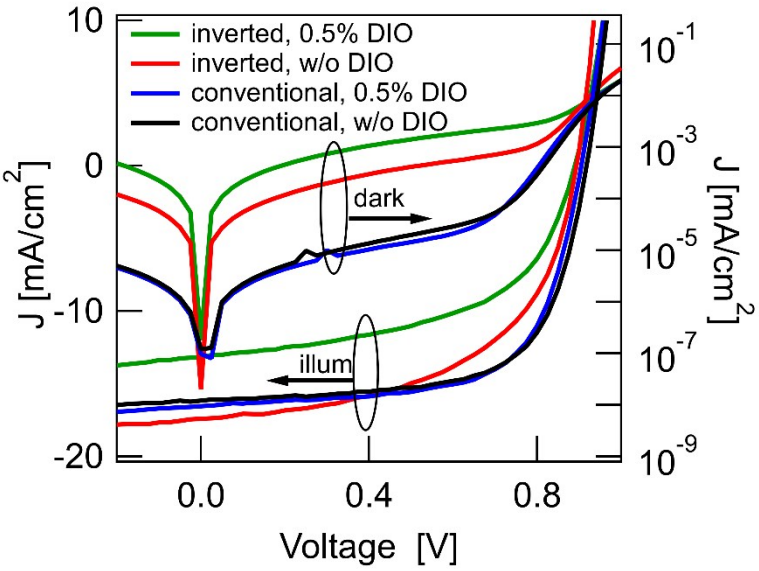

Figure S1 *J-V*-curves of PBDB-T:ITIC solar cells with and w/o additive DIO in dark and under illumination: inverted with 0.5% DIO (green), inverted w/o DIO (red), conventional with 0.5% DIO (blue), conventional w/o DIO (black).

*sperlich@physik.uni-wuerzburg.de

structure	**(n=)**	**V_{OC} [mV]**	**FF [%]**	**J_{SC} [mA cm^{-2}]**	**PCE [%]**
inverted, 0.5%DIO	10	890 (884)	54.0 (50.0)	13.2 (12.8)	6.3 (5.6±0.4)
inverted, w/o DIO	16	868 (868)	53.0 (52.4)	16.4 (15.3)	7.5 (7.0±0.3)
aged inverted, w/o DIO	11	895 (894)	54.0 (53.6)	17.4 (16.5)	8.5 (8.0±0.3)
conventional, w/o DIO	5	918 (918)	66.0 (65.0)	16.2 (14.7)	9.8 (8.9±0.9)
conventional, 0.5% DIO	10	905 (907)	65.8 (64.6)	16.5 (15.1)	9.8 (8.8±0.7)

Table S1. Photovoltaic properties for conventional and inverted PBDB-T:ITIC solar cells with or w/o DIO. Best device values and averaged values for n=5-16 devices in parenthesis.

AL thickness [nm]	**(n=)**	**V_{OC} [mV]**	**FF [%]**	**J_{SC} [mA cm^{-2}]**	**PCE [%]**
115	6	918 (916)	62.7(60.7)	16.8 (15.3)	9.6 (8.5±0.9)
100	5	918 (919)	66.2 (65.5)	16.2 (14.7)	9.8 (8.9±0.9)
90	8	918 (916)	67.8 (66.5)	12.6 (11.9)	7.9 (7.3±0.6)

Table S2. Photovoltaic properties of conventional PBDB-T:ITIC solar cells w/o DIO and with different active layer (AL) thickness. Best device values and averaged values for n=5-8 devices in parenthesis.

Annealing temp. [°C]	**(n=)**	**V_{OC} [mV]**	**FF [%]**	**J_{SC} [mA cm^{-2}]**	**PCE [%]**
70, 30 min	16	868 (868)	53.0 (52.4)	16.4 (15.3)	7.5 (7.0±0.3)
100, 10 min	8	875 (868)	58.1 (53.8)	12.6 (12.0)	6.4 (5.6±0.5)

Table S3. Photovoltaic properties of inverted PBDB-T:ITIC solar cells w/o DIO, but with 10 or 30 minutes of thermal annealing at different temperatures. Averaged values for n=8 or 16 devices in parenthesis.

Electroluminescence – EL

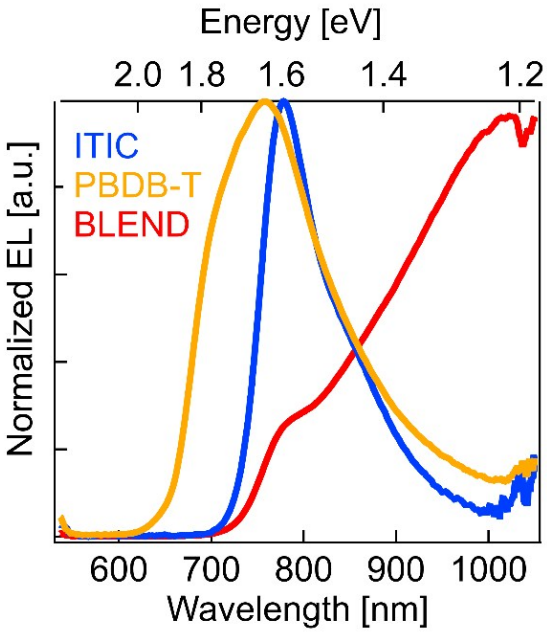

Figure S2. Normalized EL spectra of pure PBDB-T (yellow), pure ITIC (blue) and a fully processed solar cell measured as OLED under current injection (red).

Temperature Dependent V_{OC}

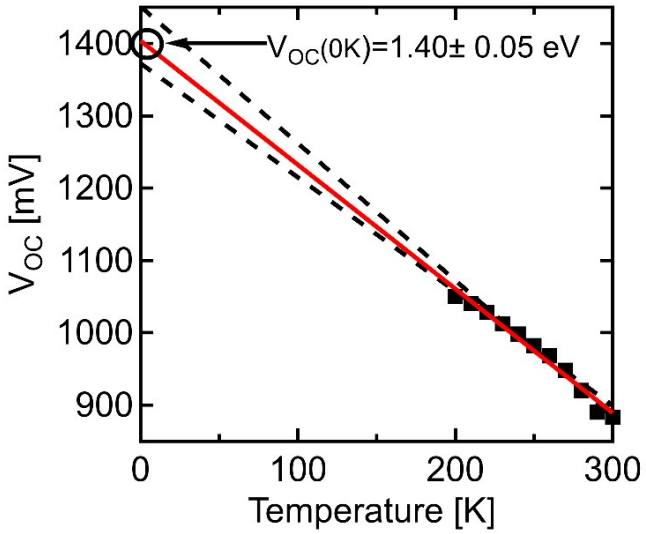

Figure S3. Inverted OSC V_{OC} temperature dependence (black dots) and linear fit (red line) with error band (black dashed lines)

Marcus Theory for Charge Transfer State Absorption and Emission

In the framework of Marcus theory, the spectral line shape of the charge transfer (CT) state absorption cross section $\sigma(E)$ times photon energy E is described by:

$$\sigma(E)E = \frac{f_\sigma}{\sqrt{4\pi\lambda kT}} exp\left(\frac{-(E_{CT}+\lambda-E)^2}{4\lambda kT}\right), \quad (1)$$

where k is Boltzmann's constant and T is the absolute temperature. E_{CT} denotes the free-energy difference between ground state and CTS and λ is the reorganization energy, associated with the CT absorption process[1,2].

The counterpart is the CT emission rate $I_f(E)$ per unit energy E:

$$\frac{I_f(E)}{E} = \frac{f_{I_f}}{\sqrt{4\pi\lambda kT}} exp\left(\frac{-(E_{CT}-\lambda-E)^2}{4\lambda kT}\right). \quad (2)$$

Both f_{I_f} and f_σ are not dependent on E and are proportional to the square of the electronic coupling matrix element. The left-hand side of Equations (1) and (2) are called the reduced absorption and emission spectrum respectively and exhibit a mirror image relationship.

Singlet and Triplet states DFT modelling

The gas-phase ground-state equilibrium geometry of the donor PBDB-T tetramer and of ITIC were optimized using Density Functional Theory at the range-separated hybrid (RSH) functional level of theory, using the ωB97X-D functional and the 6-31G(d,p) basis set for all the atomic species[3]. In order to speed up the calculations, the alkyl chains in the investigated molecules were replaced with methyl groups. The ITIC structure was taken from the crystallographic data in Ref.4. Excitation energies, oscillator strengths and absorption spectra of the two systems were then investigated by time-dependent DFT (TD-DFT) calculations within the Tamm-Dancoff approximation (TDA) [5] and employing a polarizable continuum model (PCM) [6] with a dielectric constant of ε = 4.5 in order to take the electronic polarization and the solid-state environment into account. For such calculations, we used the LC-ωhPBE [7] functional in order to resort to a screened RSH (SRSH) functional[8,9]. In this approach, ω (the exchange range-separation parameter) was optimally tuned in vacuum and set at 0.1010 $Bohr^{-1}$ for the donor and 0.0970 $Bohr^{-1}$ for the NFA, according to the "gap-tuning" procedure[10,11]. Then, solid-state effects were introduced combining the SRSH functional with PCM and following the relationship $^{1}/_{\varepsilon} = \alpha + \beta$, where $\alpha + \beta$ controls the Hartree-Fock exchange amount at the long-range domain while α quantifies the Hartree-Fock exchange amount at short-range. In our calculations, α was set at 0.2 and, by consequence, β at 0.022. Ground-state optimizations and excitation energies were obtained using the Gaussian16 code[12]. Figure S4 shows the calculated absorption spectra for a pure PBDB-T tetramer and for ITIC.

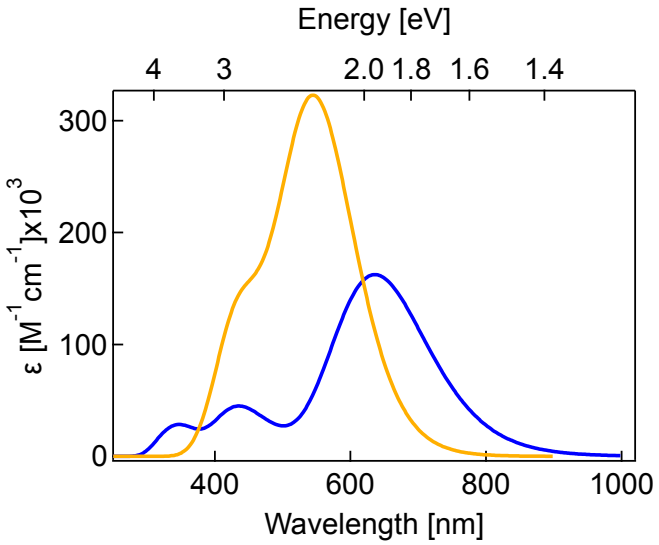

Figure S4: TDA-DFT absorption spectra of the donor PBDB-T tetramer (orange) and ITIC (blue). These spectra were obtained with SRSH LC-ωhPBE functional. By mimicking the impact of the solid-state environment, the calculations were carried out within PCM and a dielectric constant ε = 4.5 was set.

In order to corroborate PLDMR results, spin properties, including zero-field splitting (ZFS) parameters, were calculated at the DFT level of theory on an isolated ITIC molecule in a triplet ground-state with the ωB97X-D3 functional and the Def2-TZVP basis set for all the elements[13]. We also took advantage of the RIJCOSX approximation along with the Def2/J and Def2-TZVP/C

auxiliary basis set, as implemented in the ORCA 4.2.1 software[14]. In this work, we focused only on the calculation of the direct dipolar spin-spin (SS) contribution to the ZFS tensor; the components of the ***D*** tensor were evaluated using the unrestricted natural orbitals (UNO) obtained from the unrestricted Kohn-Sham orbitals, as suggested in Refs. 15,16. Spin properties are strictly related to the geometries and even small variations of the structural parameters could affect the computed values. For such reason, the ITIC X-ray crystal structure was used for the ZFS calculation, which yielded a D_{SS} of 0.024 cm^{-1} or 25.7 mT and an average spin-up – spin-down distance of 1.4-1.5 Å. As regards the intermolecular delocalized triplet exciton, for this state, we performed an OT-SRSH TDA-DFT/PCM calculation for an ITIC dimer. The dimer was taken directly from the crystallographic data reported in literature[4] and only the hydrogen atoms were optimized at the DFT ωB97X-D/6-31G(d,p) level of theory. Moreover, we were also able to estimate the e-h capture radius of 4.5Å, which can be taken as a proxy for the spin-up – spin-down distance. Since the magnetic dipole-dipole interaction should scale as r^{-3}, we estimated the *D* ZFS parameter on the ITIC dimer to be ~1 mT. These findings are in line with the results from the EasySpin calculations (*vide infra*).

Modeling of Triplets in Pure Materials by EasySpin

The magnetic resonance spectrum of a triplet can be calculated on the basis of the eigenvalues and eigenvectors obtained from the diagonalization of the spin Hamiltonian that includes the anisotropic Zeeman term and the electron dipolar term, also called zero-field splitting (ZFS) term:

$$H = g\mu_B BS + SDS$$

where g is the g-tensor related to Zeeman interaction, ***D*** is the dipolar interaction tensor, ***B*** is the magnetic field vector, ***S*** is the spin operator, and μ_B is the Bohr magneton[17,18]. The eigenvalues *X, Y* and *Z* of the ***D*** tensor are commonly expressed in terms of the ZFS parameters *D* and *E* that are defined as $D = -3/2Z$ and $E = 1/2(Y-X)$. The *D* parameter is related to the average interaction between the two unpaired spins, and therefore contains information about the mean distance of the two and thus the triplet state delocalization. The *E* parameter describes the off-axial interaction strength for systems with symmetry lower than axial. In general, there are two allowed transitions between the three triplet sublevels ($\Delta m_s = \pm 1$) that correspond to two peaks of the magnetic resonance spectrum. Both, the Zeeman and the dipolar terms in the spin Hamiltonian, however, depend on the relative orientation between the molecules and the magnetic field ***B*** and therefore, in a disordered material like an organic film, the resulting spectrum is the sum of contributions from all randomly-oriented molecules. This is commonly referred to as a powder pattern.

The PLDMR spectra of PBDB-T and ITIC thin films are shown in Figure S5. Both contain a broad spectral feature that can be assigned to localized molecular triplet excitons together with a narrow peak in the center that stems from CT TE and exciton-charge interaction. This contribution is cut and neglected for PBDB-T. The EasySpin[19] spectral simulation of the PLDMR spectrum of PBDB-T is obtained using the following ZFS parameters: D = 52.0 mT and E = 5.6 mT. The spectral simulation of the ITIC spectrum includes two sets of parameters. The first triplet, corresponding to the broader signal, has the following ZFS parameters: D = 45.5 mT and an E = 15.0 mT. The

narrow peak of the ITIC spectrum contains two contributions: a very narrow peak that, like for PBDB-T, is neglected and a less narrow peak that we assign to a delocalized triplet exciton. The simulation of this ITIC triplet state provides $D = 0.8$ mT and $E = 0$. We attribute these two triplets to a strongly localized molecular triplet exciton (broad spectrum with strong dipolar interaction) and more delocalized TE state with some CT character (narrow spectrum with weak dipolar interaction). Two TE states with slightly different energy and different delocalization are predicted by theory and detected here with magnetic resonance.

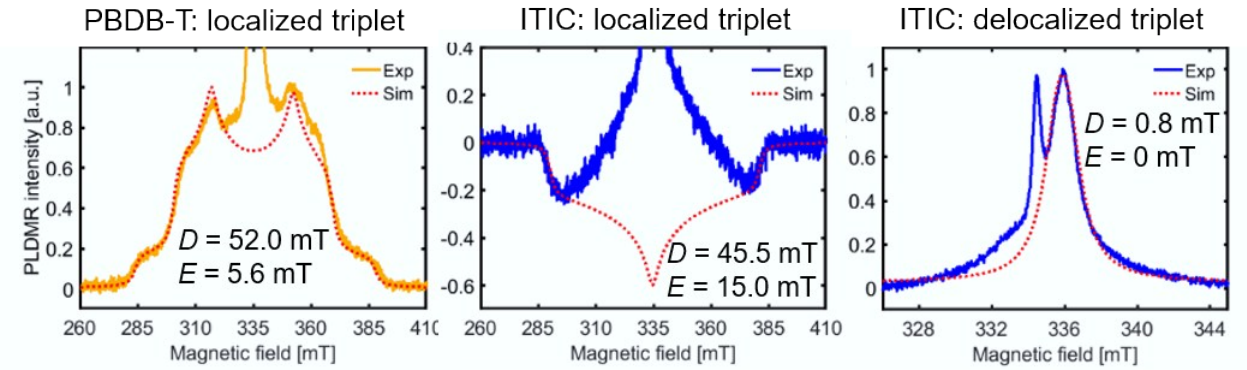

Figure S5. PLDMR spectra for PBDB-T (yellow) and ITIC (blue) triplet excitons together with spectral simulations. While the spectrum of PBDB-T and the narrow spectral feature of ITIC can be fitted quite accurately, the sign of the broad spectral features of ITIC cannot be reproduced. The peaks, shoulders and turning points are accurately determined, which is sufficient to extract TE parameters D and E. The sign and intensity of a PLDMR spectrum can however be dependent on orientation dependent rate constants and are not easily reproducible by simulation.

Supporting Information References

1. R. Gould, D. Noukakis, L. Gomez-Jahn, R. H. Young, J. L. Goodman, S. Farid. *Chem. Phys.,* 1993, **176**, 439 doi:10.1016/0301-0104(93)80253-6

2. K. Vandewal, K. Tvingstedt, A. Gadisa, O. Inganäs, J. V. Manca. *Phys. Rev. B,* 2010, **81**, 125204 doi:10.1103/PhysRevB.81.125204

3. J.-D. Chai, M. Head-Gordon. *Phys. Chem. Chem. Phys.,* 2008, **10**, 6615 doi:10.1039/B810189B

4. T. J. Aldrich, M. Matta, W. Zhu, S. M. Swick, C. L. Stern, G. C. Schatz, A. Facchetti, F. S. Melkonyan, T. J. Marks. *J. Am. Chem. Soc.,* 2019, **141**, 7, 3274 doi:10.1021/jacs.8b13653

5. S. Hirata, M. Head-Gordon. *Chem. Phys. Lett.,* 1999, **302**, 375 doi:10.1016/S0009-2614(99)00137-2

6. J. Tomasi, B. Mennucci, R. Cammi. *Chem. Rev.,* 2005, **105**, 2999 doi:10.1021/cr9904009

7. T. M. Henderson, A. F. Izmaylov, G. Scalmani, G. Scuseria. *J. Chem. Phys.,* 2009, **131**, 044108 doi:10.1063/1.3185673

8. S. Refaely-Abramson, S. Sharifzadeh, M. Jain, R. Baer, J. B. Neaton, L. Kronik. *Phys. Rev. B,* 2013, **88**, 081204 doi:10.1103/PhysRevB.88.081204

9. Z. Zheng, D. A. Egger, J.-L. Brédas, L. Kronik, V. Coropceanu. *J. Phys. Chem. Lett.,* 2017, **8**, 14, 3277 doi:10.1021/acs.jpclett.7b01276

10. T. Stein, L. Kronik, R. Baer., *J. Am. Chem. Soc.,* 2009, 131, 2818 doi:10.1021/ja8087482

11. T. Stein, H. Eisenberg, L. Kronik, R. Baer., *Phys. Rev. Lett.,* 2010, **105**, 266802, 1 doi:10.1103/PhysRevLett.105.266802

12. Gaussian16 Revision A.03, M. J. Frisch, G. W. Trucks, H. B. Schlegel, G. E. Scuseria, M. A. Robb, J. R. Cheeseman, G. Scalmani, V. Barone, G. A. Petersson, H. Nakatsuji, X. Li, M. Caricato, A. V. Marenich, J. Bloino, B. G. Janesko, R. Gomperts, B. Mennucci, H. P. Hratchian, J. V. Ortiz, A. F. Izmaylov, J. L. Sonnenberg, D. Williams-Young, F. Ding, F. Lipparini, F. Egidi, J. Goings, B. Peng, A. Petrone, T. Henderson, D. Ranasinghe, V. G. Zakrzewski, J. Gao, N. Rega, G. Zheng, W. Liang, M. Hada, M. Ehara, K. Toyota, R. Fukuda, J. Hasegawa, M. Ishida, T. Nakajima, Y. Honda, O. Kitao, H. Nakai, T. Vreven, K. Throssell, J. A. Montgomery, Jr., J. E. Peralta, F. Ogliaro, M. J. Bearpark, J. J. Heyd, E. N. Brothers, K. N. Kudin, V. N. Staroverov, T. A. Keith, R. Kobayashi, J. Normand, K. Raghavachari, A. P. Rendell, J. C. Burant, S. S. Iyengar, J. Tomasi, M. Cossi, J. M. Millam, M. Klene, C. Adamo, R. Cammi, J. W. Ochterski, R. L. Martin, K. Morokuma, O. Farkas, J. B. Foresman, and D. J. Fox, Gaussian, Inc., Wallingford CT (2016)

13. Y. S. Lin, G. D. Li, S. P. Mao, J. D. Chai. *J. Chem. Theory Comput.,* 2013, **9**, 263 doi:10.1021/ct300715s

14. F. Neese. *WIREs Comput. Mol. Sc.,* 2012, **2,** 73, doi:10.1002/wcms.81

15. S. Sinnecker, F. Neese. *J. Phys. Chem. A*, 2006, **110**, 12267 doi:10.1021/jp0643303

16. A. Lunghi, F. Totti. *J. Mater. Chem. C*, 2014, **2**, 8333 doi:10.1039/C4TC00847B

17. S. Richert, C. E. Tait, C. R. Timmel. *J. Magn. Reson*., 2017, **280**, 103 doi:10.1016/j.jmr.2017.01.005

18. C. Hintze, U. E. Steiner, M. Drescher. *Chem. Phys. Chem.,* 2017, **18**, 1, 6 doi:10.1002/cphc.201600868

19. S. Stoll, A. Schweiger. *J. Magn. Reson.,* 2006, **178** (1), 42 doi:10.1016/j.jmr.2005.08.013